Coarse-grained molecular-dynamics simulations of nanoparticle diffusion in polymer nanocomposites

Coarse-grained Molecular-dynamics Simulations of Nanoparticle Diffusion in Polymer Nanocomposites

I.V. Volgin[1], S.V. Larin[1], A.V. Lyulin[1,2], S.V. Lyulin[1]

[1]*Institute of Macromolecular Compounds, Russian Academy of Sciences, Bolshoj pr. V.O., 31, 199004, Saint Petersburg, Russia*

[2]*Group Theory of Polymers and Soft Matter, Department of Applied Physics, Technische Universiteit Eindhoven, 5600 MB, Eindhoven, The Netherlands*

Keywords: coarse-graining, nanoparticle dynamics, molecular dynamics simulations

***Corresponding author, e-mail: Sergey V. Lyulin, s.v.lyulin@gmail.com.**

Abstract

Molecular-dynamics simulations have emerged as an effective tool to characterize polymer systems. Molecular level effects (even on microsecond time scales) are nowadays well reproduced by atomistically detailed models. Beyond this, further insights into the properties of the polymer system at a mesoscopic level can be gained by resorting to simulations based on appropriate coarse-grained models. However, reducing the number of degrees of freedom during the coarse-graining procedure may have a significant impact on atomistic level effects. A common example is the overall enhancement of the diffusive motion of polymer chains in coarse-grained simulations, which arises from the reduced friction of the coarse-grained beads. In the present work we investigate this well-known effect and study how the diffusive properties of the nanoparticle are affected by the coarse-graining procedure. To this end, we apply iterative Boltzmann inversion to develop two coarse-grained models of a nanocomposite based on the thermoplastic polyimide R-BAPB, containing a single fullerene C_{60} nanoparticle. By changing the size and, correspondingly, the total number of coarse-grained beads in each polymer chain, we can control the effect of chemical detalization on various phenomena. We exploit this idea to study the influence of the degree of detalization of polymer chains on their structural properties as well as on the diffusive properties of the fullerene nanoparticle, whose detalization is kept fixed. Although the structural properties of the coarse-grained systems are in good agreement with those of the fully atomistic system, the nanoparticle diffusion is significantly affected by the local chain structure. In particular, we find that the coarse-graining of the polymer chains on the length scale of the nanoparticle size leads to a full suppression of the subdiffusive regime observed in the fully atomistic system.

1. Introduction

The properties of polymer systems originate from the hierarchy of their different time and length scales. A better understanding of how microscopic mechanisms taking place at the atomistic level give rise to the observed macroscopic effects would open new routes for the rational design of novel materials with advanced properties. Over the past decades, computer simulations have emerged as a powerful tool to solve this fundamental problem. Starting from the simple freely-jointed and bead-spring models [1], we are nowadays able to benefit from the highly detailed simulations on time scales approaching the experimental ones. Indeed, the rapid increase of the computational performance of modern supercomputers allows one to perform computer simulations on the microsecond time scale within «united-atom» [2-5] and even atomistically-detailed models [6-12]. However, even such long-time simulations are not long enough to capture all the macroscopic effects in polymers and in polymer nanocomposites (PNCs), i.e., polymer crystallization, kinetics of nanoparticle aggregation, etc. Moreover, in the framework of atomistically-detailed models, significant computational efforts are still required to understand the properties of well-equilibrated, highly-entangled polymer systems (especially of those with rather complex chemical structures, such as heterocyclic polymers). In view of this, there is a pressing need to develop suitable computational frameworks allowing one to attain sufficiently long times and sufficiently large length scales.

In the above context, recent years have seen a rapid development of multiscale simulation approaches aimed at linking together the different time and length scales, in order to correctly predict the properties of complex polymers [13]. Among the most commonly used and effective tools are various coarse-graining (CG) techniques [14]. These techniques allow one to access much larger time and length scales due to the effective averaging over the microscopic details of the underlying atomistic system. In practice, the averaging process is performed by merging groups of atoms into CG beads. A major challenge in this context consists in attaining a suitable balance between the computational efficiency characteristic of simple polymer models and the high degree of detalization achieved in fully atomistic simulations.

Much effort in this field has been put into the understanding of the influence of the degree of the polymer coarse-graining on the structural, rheological and thermal properties of different bulk polymers,

such as polystyrene (PS), polyisoprene (PI), polyethylene (PE), poly(3-hexylthiophene) (P3HT), sulfonated polyetherketone (sPEEK) and even aromatic polyimides [15-24]. Concerning the effects governing structural properties, Harmandaris et al. have studied the influence of the effective-bead mass on the structural properties of PS [20, 21]; Tripathy et al. examined the critical level of coarse-graining and the effect of a sequence of CG beads in a polymer chain on structural properties of sPEEK [15]. Ohkuma and Kremer investigated the effect of pressure correction on the structural properties of PI [22]. Pandiyan et al. studied the influence of the degree of coarse-graining on the mechanical properties of aromatic polyimides [16]. The polymer dynamical properties were also addressed in the above studies. A common feature was the observation of an overall enhancement of diffusive transport introduced by the CG procedure. This enhancement was attributed to the much softer CG interaction potentials, resulting in the need of applying a suitable scaling procedure to match the dynamical properties of both the original and the CG system [25]. In this context, various features have been the object of vivid discussions, notably the dependence of the scaling factor on the chain length [17, 21] or on temperature [24]. Particularly strong efforts were devoted to reproducing the AA dynamics correctly by increasing the friction of the coarse-grained beads [16].

In spite of the considerable attention paid to the development of CG polymer models, the computational design of high-performance specific materials for modern industry calls for the study of more complex systems, namely, polymer nanocomposites. Nowadays, PNC filled with carbon nanoparticles (nanotubes, graphene or fullerene) are becoming widely employed in various industrial applications. Among different polymers heterocyclic ones (for example: polythiophenes, polybenzimidazole, aromatic polyimides etc.) represent a promising class of materials which may be utilized as binders for advanced PNC for solar cell applications, fuel cell membranes and optoelectronics. [26, 27] Properties of such systems are largely controlled by the complex microstructure, which is typically formed during the nanoparticle diffusion. Due to the rapid development of the modern industry significant efforts are made to understand better PNC properties from the standpoint of the complexity of polymer chemical structure or nanoparticle induced effects. Considerable understanding may be achieved while employing computer simulations to study such systems, especially within the coarse-grained simulations. Nevertheless, the impact of the underlying coarse-grained models on the relevancy of the simulation results are nowadays less understood, thus limiting their application.

The properties of PNC are controlled not only by the chemical structure of their components (polymer matrix and filler nanoparticles), but also by the specific polymer-filler nanoparticle interactions [28-35]. This imparts additional complexity into the problem, especially when suitable CG models are to be developed. Moreover, since the polymer-nanoparticle interactions and the associated dynamics control the rheology and multi-scale mechanics of the PNC, among the key problems is understanding the variation of dynamical properties of the filler nanoparticles during the coarse-graining procedure. Though there exist numerous works on structure and dynamics of bead-spring nanocomposites with varied polymer-nanoparticle interactions [28-35], there are no studies considering nanoparticle diffusion in polymers within chemically specific CG models of different detalization.

When simulating nanoparticle diffusion, it should be taken into account that the nanoparticle dynamics is a rather complicated process characterized by different diffusion regimes, i.e., ballistic, subdiffusive and normal diffusive. In general, the characteristics of these three regimes (including typical crossover times) depend on the relaxational properties of the embedding polymer matrix. Moreover, since nanoparticle diffusion has been shown to be scale-dependent [36, 37], the characteristics of the nanoparticle motion in a polymer matrix depend on the ratio between the size of the filler particle and the most relevant length scales of the polymer system.

Within the range of length scales associated with the subdiffusive regime of the nanoparticle, the chemical heterogeneity of polymer chains plays the most important role, since this heterogeneity is responsible for the local viscosity felt by the nanoparticle. However, in any coarse-grained simulations, the level of detail of the chemical structure is always reduced. Establishing how the degree of coarse-graining of the polymer affects the diffusive properties of the nanoparticles in PNC on various length scales of diffusion is crucial to develop suitable coarse-grained PNC models. The answer to this question will provide the information about the critical length scale and the necessary degree of coarse-graining which is needed to preserve the local effects.

In this paper we address the above problem by studying the diffusion of the nanoparticle in the framework of two PNC models differing in their degree of coarse-graining. In both models, the nanoparticle is modeled as a single coarse-grained bead. We use these CG models to simulate the diffusion of a single fullerene C_{60} in the melt of R-BAPB high-performance thermoplastic crystallizable polyimide based on 1,3-bis-(3,3′,4,4′-dicarboxyphenoxy)benzene (dianhydride R) and 4,4′-bis-(4-

aminophenoxy) biphenyl (diamine BAPB), This polymer system has a high industrial impact, and has already been the object of previous studies by ourselves [6-10, 38].

The complex chemical structure of the R-BAPB polyimide makes it a promising object to be used while investigating the role of the local chain structure and its coarse-graining on the nanoparticle diffusion. To minimize the number of parameters which may contribute to the nanoparticle diffusion, a simple nanoparticle should be utilized as a model diffusive object. Due to its spherical symmetry, small sizes and electrical neutrality, fullerene C_{60} seems to be the most reasonable candidate among other carbon nanoparticles, being typically used in modern nanocomposites.

In the present study we focus our attention on the structural and dynamical properties of the PNC, and compare CG simulation results with those obtained previously in the framework of fully-atomistic molecular-dynamics (MD) simulations of the same system [38].

The paper is organized as follows. In Section 2 we describe the simulation models and the details of the applied coarse-graining procedure. In Section 3 we discuss the results for the structural properties of the polymer and for the diffusive properties of both the polymer chains and the nanoparticle. In this context, special attention is paid to the nanoparticle diffusion in the framework of two different CG models. Finally, the general conclusions are summarized in Section 4.

2. Simulational models and methods

We investigate the translational diffusion of the buckyball fullerene C_{60} in the melt of polyimide R-BAPB [38]. This polyimide has rather large monomer units with a complicated chemical structure and an associated contour length about 4 nm. Therefore, this system seems *a priori* very well suited to discuss the issues mentioned in the Introduction. Despite the high degree of heterogeneity of R-BAPB polymer chains, there are fortunately no highly polarizable groups in its structure, and the dipole-dipole interactions induced by the presence of partial charges are rather weak. Thus the CG models discussed below were developed on the basis of a fully atomistic model where partial charges had been set to zero.

To investigate the influence of the polymer coarse-graining on the fullerene diffusion we developed two coarse-grained models. The first model, CG1, retains a high level of detail of the underlying chemical structure, while the second model, CG2, involves a larger degree of coarse-graining,

see Fig.1. The CG1 model is characterized by the explicit presence of an oxygen hinge group and a larger number of CG particles, representing flat fragments (consisting of two phenyl rings) of the polymer chains. These important differences allowed us to control the degree of chemical complexity of the R-BAPB polymer chains in each of the two CG models. In both models, the fullerene was implemented as a single CG bead (see Fig. 1).

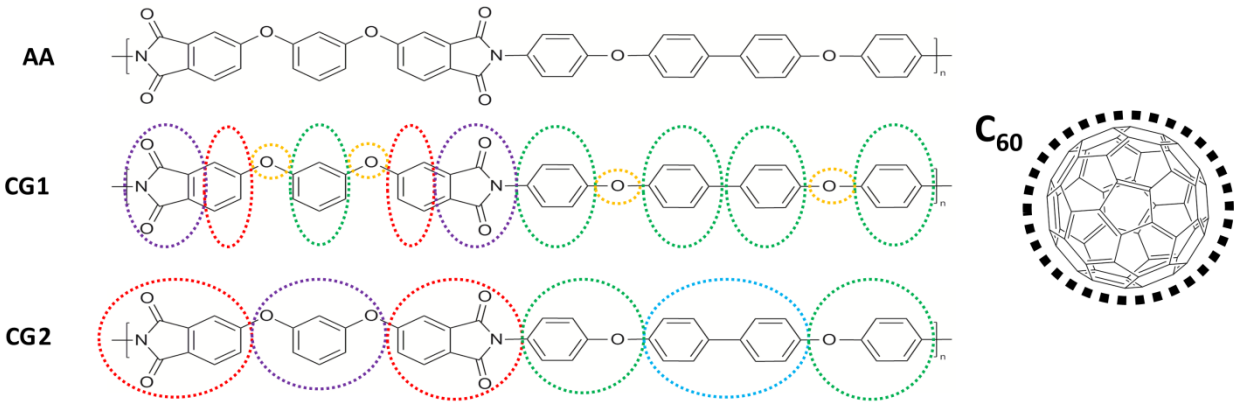

Fig. 1. Three different representations of the chemical structure of the fullerene C_{60} and the monomer unit of R-BAPB polyimide, namely, the atomistic model (AA) used in [38] and the two coarse-grained models, CG1 and CG2. Dashed circles represent the effective coarse-grained particles.

In each model, the interaction potentials between the different CG particles were calculated with the Iterative Boltzmann Inversion (IBI) technique. To this end, trajectories that had been previously computed within AA simulations were used as an input [38]. To perform the iterative procedure, the VOTCA toolkit was used [39]. This tool had already been successfully applied to the coarse-graining of aromatic polyimides [16].

Assuming that the coarse-grained degrees of freedom prescribed by our models are independent, the total energy of the system, U_{total}^{CG}, may be separated into two terms, i.e. the bonded part, U_{bonded}^{CG}, and the non-bonded part, $U_{non-bonded}^{CG}$:

$$U_{total}^{CG} = \sum U_{bonded}^{CG} + \sum U_{non-bonded}^{CG}. \quad (1)$$

In the first stage of the IBI procedure, the initial CG potentials for each pair of beads were derived from their target distributions P_{target}, obtained from the corresponding atomistic trajectory. To this end we used 1μs-long trajectory obtained in our earlier studies on the corresponding atomistic system [38].

Taking the target distributions as reference, a separate IBI iteration procedure was performed to obtain the non-bonded and the bonded potentials. In order to obtain a CG potential able to reproduce the target property with sufficiently high accuracy, a correcting procedure is applied on each iteration. In the *n+1*-th iteration step, the potential $U^{(n)}$ from the *n*-th iteration evolves into a new form $U^{(n+1)}$ prescribed by the following algorithm:

$$U^{(n+1)} = U^{(n)} + k_B T \ln \frac{P^{(n)}}{P_{ref}}, \quad (2)$$

where $P^{(n)}$ refers to the pair distribution function obtained in the *n*-th iteration.

A set of interaction potentials was optimized in order to correctly reproduce the target properties of the original atomistic system, such as the radial distribution functions for the separation distance between randomly chosen pairs of CG beads, the distributions of the bond lengths and those of the valence angles. In a first stage the iterative procedure was carried out to obtain the non-bonded potentials. At the same time, the potentials for the bonds, angles and dihedrals were obtained from the corresponding target distributions via direct Boltzmann inversion, $U(r) = -k_B T \ln P_{ref}(r)$. The iteration procedure was performed until a minimal difference between the successive estimates for the pair distribution functions and their target counterparts was attained. All the non-bonded interaction potentials were assumed to be independent, except for the case of potentials including a common bead (e.g. “A-B” and “B-C”). In this case such potentials were derived on different iterations. Having obtained the tabulated non-bonded potentials, a new iteration procedure was applied in the next step to obtain tabulated bonded potentials between the CG beads of the polymer chain. At this stage, Ryckaert-Bellemans functions were used for the torsional potentials [40]:

$$V_{rb}(\phi_{ijkl}) = \sum_{n=0}^{5} C_n (\cos(180° - \phi))^n. \quad (2)$$

The parameters for the dihedral potentials were obtained by fitting the corresponding potentials obtained from dihedral angle distributions using Boltzmann inversion. The dihedral angle distributions were calculated from the atomistic simulations. The potentials describing the interaction between the polymer beads were derived independently from the polymer-nanoparticle potentials. To derive the non-bonded potentials describing the interaction between the polymer beads and the nanoparticle, we performed an additional IBI procedure. The resulting potentials were used to perform the microsecond-

long MD simulations of two CG systems containing 1 fullerene and 27 polymer chains with degree of polymerization $N_p = 8$ (Fig. 2).

In order to provide a comprehensive verification of the developed coarse-grained models we have compared the radial distribution functions, both between the polymer beads and between the polymer beads and the fullerene. Additionally, we have also examined the correlations between the bond lengths, valence angles and dihedral angles of the polymer chains in each coarse-grained model. These results were compared with those obtained from the reference atomistic simulations. A good agreement is observed between the results based upon both CG models and those for the reference atomistic model, which provides the necessary arguments about the validity of the developed CG models. For more details we refer the reader to the corresponding sections of the Supporting Information (see Figs. 1S-10S).

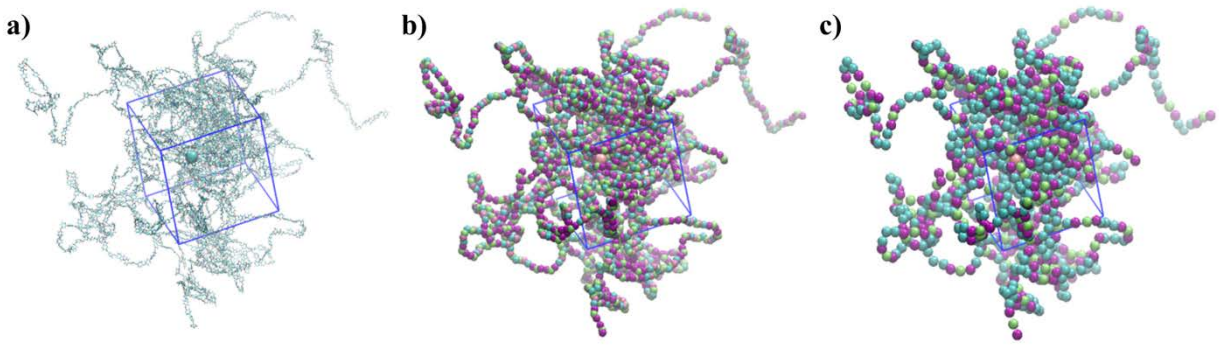

Fig. 2. Snapshot of a single system configuration in the three different representations (a) atomistic and coarse-grained (b) CG1 and (c) CG2. The blue simulation box is also shown.

The MD simulations were performed in the NpT ensemble with the same parameters as in our previous studies, $p = 1\ bar$, $T = 600\ K$ [38]. A Parrinello-Rahman barostat ($\tau_p = 5.0\ ps$) and a Nose-Hoover thermostat ($\tau_T = 1.0\ ps$) were used to keep the temperature and pressure values constant. Both for the CG1 and for the CG2 models, the initial condition was generated from a single configuration given by a snapshot of the time evolution of the fully atomistic system. This snapshot was obtained from the AA simulations performed in our previous study [38] and corresponds to the randomly chosen instant t=120 ns.

For both CG models we have investigated (i) the structural properties of the polymer chains; (ii) the dynamic properties of both the polymer chains and the nanoparticle; (iii) the details of the subdiffusive dynamics of the nanoparticle.

3. Results

3.1. Structural properties of the polymer chains in the melt

As in our previous study, the polymer system was considered to be equilibrated once the average size of the polymer chain had reached a stationary value. This value turned out to be in agreement with previous theoretical estimates [6-10, 38]. The time-dependence of the end-to-end distance $\boldsymbol{H_{end-to-end}}$ and of the chain radius of gyration $\boldsymbol{R_g}$ are shown in Fig. 3.

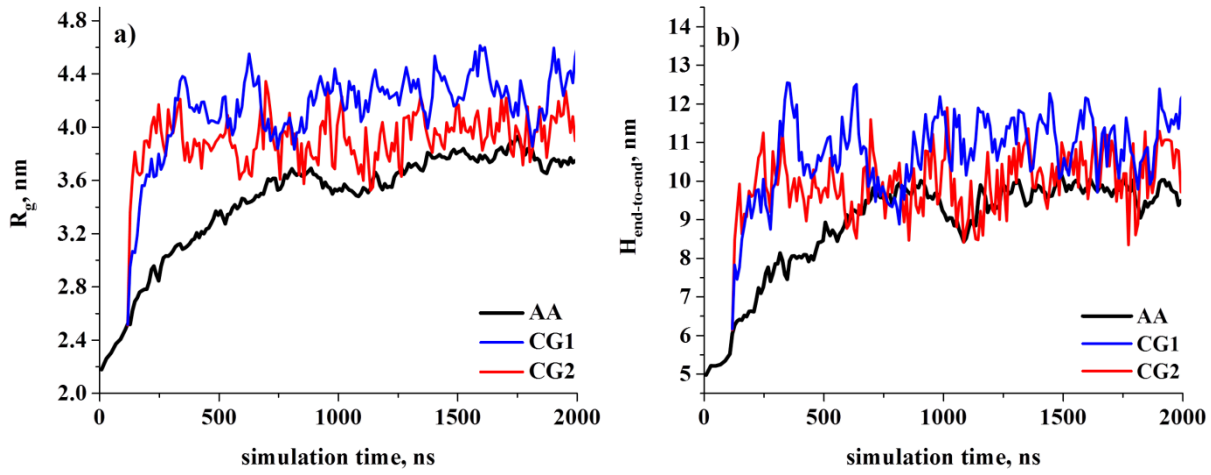

Fig. 3. Time evolution of the radius of gyration R_g (a) and of the end-to-end distance $H_{end-to-end}$ (b) of polyimide chains in the melt. Black curves for the AA model have been taken from our previous study [38].

As seen in Fig. 3, increasing the degree of coarse-graining of the polymer chains associated with the CG2 model leads to larger fluctuations of the R_g and $H_{end-to-end}$ values. This is probably related to the accelerated conformational dynamics in this CG system. However, within the reported error bars, the average values of R_g and $H_{end-to-end}$ were found to be in good agreement with the results of the corresponding atomistic simulations (in spite of the difference in the presence of the oxygen hinge group and in the number of CG particles representing the flat chain fragments in each CG system, cf. Table 1).

	CG1	CG2	AA
R_g, nm	4.2±0.3	3.9±0.2	3.7±0.1
$H_{end\text{-}to\text{-}end}$, nm	11±1	10±1	9.6±0.4
density, kg/m^3	1216±11	1117±17	1207±5

Table 1. Structural properties of the three systems studied.

On the other hand, the decrease in the density of the CG2 system (by about 8% with respect to the fully-atomistic system) is due to the effective increase in the excluded volume of the flat fragments, which were assumed to be spherically symmetric in the CG systems. We also performed an additional pressure correction to the non-bonded potentials describing the interaction between the polymer beads in the CG2 model. This was done to investigate the influence of a difference in density on the dynamical behavior of the nanoparticle in the nanocomposite. The obtained results are discussed at the end of Section 3.3.

3.2. Dynamic properties of the polymer chains and the nanoparticle.

To characterize the diffusive properties of both the polymer chains and the nanoparticle, the corresponding mean-squared displacements (MSDs) have been calculated,

$$< \Delta r^2 > \; = \; < \left(\vec{r}(t_0 + \Delta t) - \vec{r}(t_0)\right)^2 > \qquad (3)$$

The time dependence of the MSD for the center-of-mass of each polymer chain (averaged over all chains) and for the fullerene in different systems is presented in Fig. 4. As it can be seen, all the curves display three different regimes, described by the equation $< \Delta r^2 > \sim \Delta t^a$, namely, ballistic ($a = 2$), subdiffusive ($0 < a < 1$), and normal diffusive ($a = 1$).

The MSD curves for both CG models and for the AA model are essentially the same in the ballistic regime (corresponding to a picoseconds timescale), since all the systems have similar static structural properties. However, at larger times the dynamical properties display significant differences.

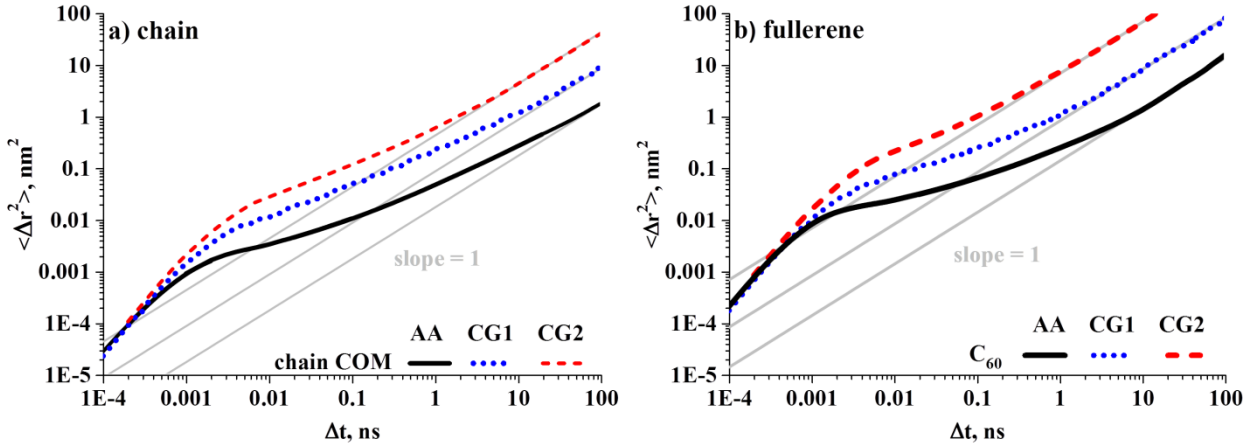

Fig. 4. Time dependence of the MSD of the set of polymer chains (obtained by averaging over the center-of-mass motions of all chains) (a) and of the fullerene center-of-mass (b). The MSD curves for the AA model have been taken from our previous study [38].

Typically (and not surprisingly) CG models exhibit faster dynamical behavior when compared to the original atomistic system. The reduced number of degrees of freedom in the coarse-grained systems yield softer interaction potentials with lower energetic barriers, leading to the overall reduction of the effective friction felt by the coarse-grained particles and, correspondingly, to enhanced diffusion.

In this sense, one may argue that the enhanced diffusion in CG systems may correspond to the diffusion in the atomistic simulations at some temperature exceeding that which was initially used to parameterize the CG model. However, it should be taken into account that the temperature shift may be not essentially the same for all the components of the system, especially in nanocomposites (see Fig. 12S in the Supporting Information).

Recently, to overcome the observed effects an energy-renormalization procedure was suggested, which provides better temperature transferability of the coarse-grained models [41, 42].

Typically, the reason for the difference in mobility is ascribed to the fact that the physical time in the coarse-grained system and the original time in the atomistic system have different physical meanings [24]. In this view, if one aims to retrieve dynamical properties from CG simulations, the coarse-grained time scale should be suitably rescaled in terms of the time scale of the original atomistic system. [14, 16-18, 20, 21, 25] A satisfactory correspondence can be obtained if the time-scale in the CG simulations is reduced by a suitable scaling factor. In our case, we shall define the latter as the ratio between the MSD

computed from the CG model at hand and the MSD computed from AA simulation trajectories. Displayed in Fig. 5 is the time evolution of this ratio in the two CG systems, both for the center-of-mass motion of the polymer chains and for the motion of the fullerene.

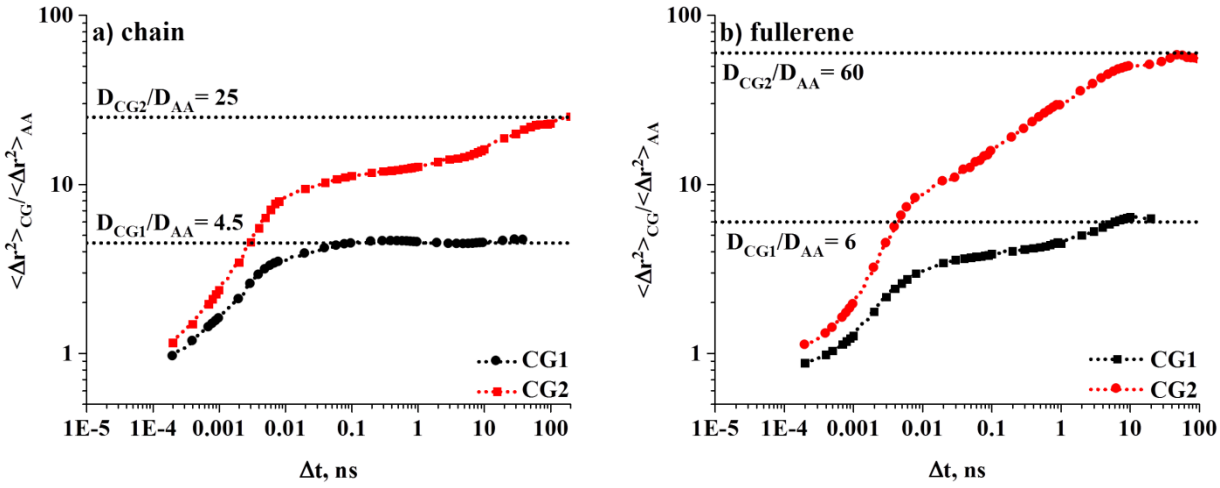

Fig. 5. Time evolution of the MSD ratio for the set of polymer chains (a) and for the fullerene (b). The dotted lines are guides to the eye.

As it can be seen, some kind of a plateau is observed at intermediate time-scales (Fig. 5a). This may be associated with the different nature of the time dependence of the MSD functions of the polymer centers-of-mass in two models (CG2 and AA). Indeed, from the Fig. 4a one may see that in the atomistic simulations the normal diffusion regime begins on the time scales around Δt = 100 ns, while in the CG1 model this regime is observed already at Δt = 20 ns. Finally, for the CG2 model this occurs even earlier - at the time-scales of 5 ns. In this case, the absence of an additional plateau on the curve in Fig. 5a for the CG1 model indicates a greater similarity of the MSD function for this model and the MSD function for atomistic simulations. On the other hand, the appearance of an intermediate plateau in the CG2 model may be associated with a faster emergence of the normal diffusion regime due to the general acceleration of the relaxation processes in the coarse-grained system.

Constant scaling factors are indeed recovered in the long-time limit, where the Stokes-Einstein relation ($< \Delta r^2 > \sim t$) holds, thus a good correspondence between the CG and atomistic system can be obtained via the time scaling $\tau_{CG} = \frac{D_{CG}}{D_{AA}} \tau_{AA}$ [25], where D_{CG} and D_{AA} denote the diffusion coefficients respectively obtained for the CG system at hand and for the AA system. The values of these diffusion coefficients were computed from the corresponding slopes of the MSD curves in the normal diffusive

regime. Note that the scaling factors obtained for the CG2 model are much larger than for the CG1 model. This is a consequence of the higher degree of coarse-graining in this model.

3.3. Subdiffusive dynamics of a nanoparticle

As already mentioned, the validity of the scaling factors obtained in Section 3.2 is restricted to the long-time regime. For intermediate time scales (corresponding to the subdiffusive regime), much less is known about the computation of suitable scaling factors. This problem is of high practical importance, but for PNC systems it is also rather intricate due to the complex interplay between the polymer dynamics and the nanoparticle motion.

In particular, from the scaling approach developed by Cai *et al.* [36], one can easily conclude that the above problem is complicated by the fact that, on intermediate time scales, the diffusional properties of the nanoparticle depend on the local viscosity of the polymer chain segments, whose size is comparable with that of the nanoparticle. Moreover, the ratio between the characteristic size of the nanoparticle and the relevant length scales of the polymer system (e.g., the radius of gyration R_g or the entanglement length) determines the time scales that are important for the dynamics.

Indeed, our previous results strongly suggest that the nanoparticle motion is coupled to the translational motion of some chain fragments, whose size is comparable with that of the diffusing nanoparticle [38]. This effect presumably gives rise to the onset of a transient subdiffusive regime ($< \Delta r^2 > \sim t^a, 0 < a < 1$) observed at intermediate times. It also turns out that the respective MSD curves of the fullerene and of the polymer flat fragment fall onto each other in the subdiffusive regime, presumably as a result of a strong coupling between the motion of the nanoparticle and that of the polymer segment (cf. Fig. 6).

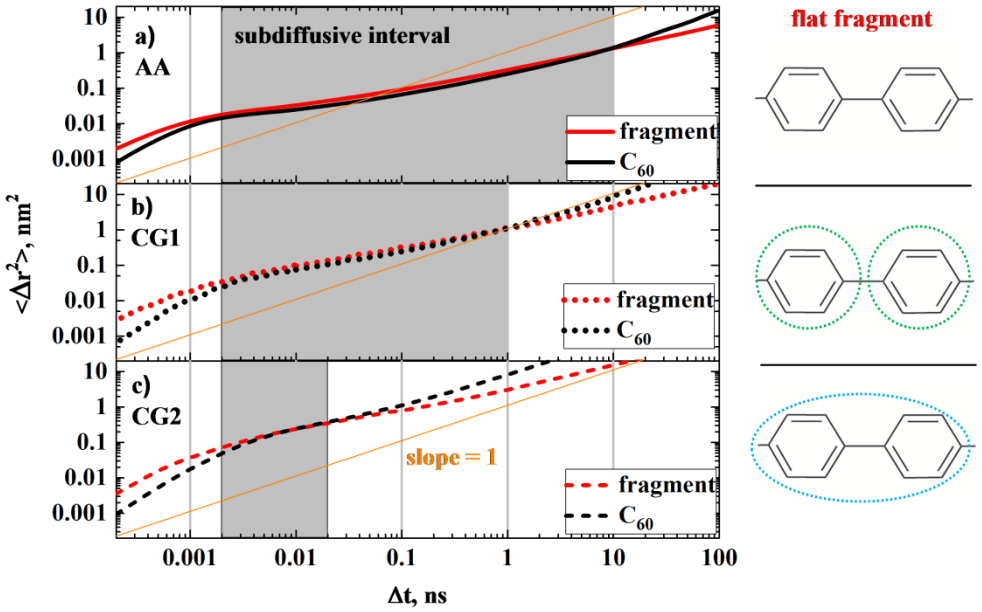

314

315 **Fig. 6.** Time-dependence of the MSD functions of the fullerene (black lines) and of the flat fragments of
316 R-BAPB chains (red lines) respectively obtained from the fully-atomistic representation used in [38] (a)
317 and from the coarse-grained representations CG1 (b) and CG2 (c). The type of polymer flat fragment in
318 each system is shown on the right. The dashed circles depict the coarse-grained particles representing the
319 chosen flat fragments. Orange lines are guides to the eye which represent the linear MSD dependence in
320 the normal diffusive regime. Gray regions correspond to the observed subdiffusive regimes.

321 As seen in Fig. 6, the width of the time interval corresponding to the subdiffusive regime is
322 strongly shortened when the degree of detalization of the polymer chains is decreased. The strongest
323 effect is observed in the CG2 system, where oxygen hinge groups are treated implicitly and the flat chain
324 fragments (approximately equal in size to the fullerene nanoparticle) are replaced by a single coarse-
325 grained bead. Moreover, in the CG1 system the MSD functions of the fragment and the fullerene match
326 each other rather well on a length scale of 1 nm, as it is also the case in the fully atomistic system.
327 However, this is not the case for the CG2 system, where the intersection point of the MSD curves is
328 shifted towards shorter length scales. Thus, on intermediate and large length scales, the CG1 model turns
329 out to be the more appropriate one for capturing the local dynamics of the fully atomistic system. In this
330 regard, it should be mentioned the existence of the more sophisticated approaches aimed on preserving
331 such local effects completely by parameterizing corresponding CG models via Mori–Zwanzig formalism.
332 [43, 44]

As already anticipated, we have additionally investigated the fullerene diffusion upon performing a pressure correction on the bead-bead polymer interaction potentials corresponding to the CG2 model. This pressure correction was performed with the aim of increasing the average density of the CG2 system until the density value of the atomistic system had been reached (recall that, according to Table 1, the relative difference in density before implementing the pressure correction was about 8%). Displayed in Fig. 7 is a comparison for the time evolution of the MSD with and without pressure correction. As one can see, differences in behavior are rather small. This suggests that, when it comes to reproducing the properties of the atomistic system, (moderate) density effects are not as important as the specific coarse-graining procedure.

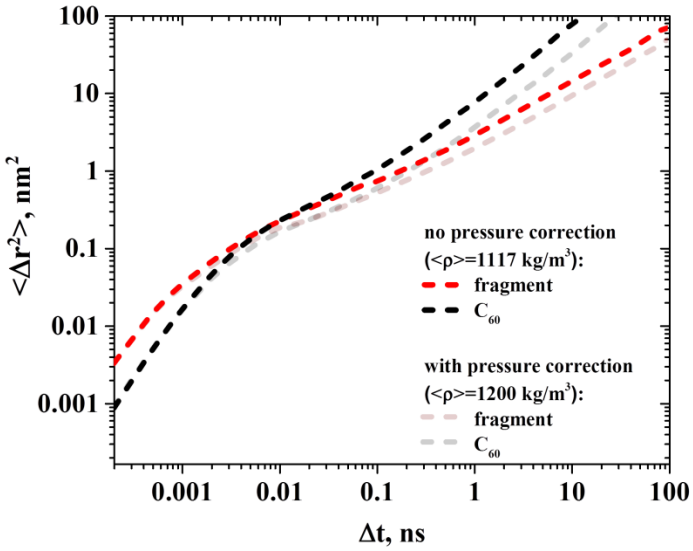

Fig. 7. MSD functions of the fullerene (black lines) and of the flat fragments of R-BAPB chains (red lines) in the CG2 system simulated with potentials obtained with and without pressure correction.

Finally, we note that the above results emphasize the important role played by the local chemical structure of a polymer chain for the subdiffusive dynamics of the nanoparticle, especially on length scales comparable with the nanoparticle size. In this sense, further elimination of the details of the chemical structure of the polymer chains should lead to a complete suppression of the subdiffusive regime.

4. Conclusions

The structural and dynamic properties of R-BAPB/C_{60} nanocomposites have been investigated by means of microsecond-long CG MD simulations. To this end, two CG models have been used,

corresponding to different degrees of coarse-graining of the polymer chains. By playing with the explicit presence of an oxygen hinge atom and by varying the number of the CG particles representing the flat chain fragments, we have investigated how the degree of the coarse-graining affects the structural and dynamical properties of the nanocomposite components.

Despite the acceleration of the overall dynamics in the coarse-grained systems, the structural properties (density and the chain size) of the polymer chains in the coarse-grained systems remain almost unchanged with respect to the original atomistic representation. However, larger fluctuations of the chain size are observed. This enhancement of fluctuations is probably due to the significant acceleration of the conformational dynamics of the polymer chains.

Furthermore, by comparing the MSD curves respectively obtained from the CG models and from the atomistic representations of the fullerene and the chain fragment, we have investigated how the subdiffusive nanoparticle dynamics depends on the details of the local structure of the polymer chains. We have focused our attention on the coupling between the flat segments and the fullerene, which had already been shown to lead to subdiffusive dynamics of the nanoparticle in atomistic simulations [38]. We have studied this effect in coarse-grained PNC systems with different degree of the chemical detalization of the polymer chains. We conclude that the subdiffusive nanoparticle dynamics is particularly sensitive to the degree of chemical «heterogeneity» of the polymer chains on length scales comparable with the nanoparticle size.

More specifically, the changes in the number of the coarse-grained particles in the flat chain fragment allow one to control the duration of the subdiffusive dynamics by changing the availability of the attractive centers in the polymer chains slowing down the nanoparticle diffusion. Thus, our results may be considered as a chemically specific example of the influence of the «polymer-nanoparticle» interactions on the dynamical properties of the nanofiller in a polymer nanocomposite. This provides further support for the scale-dependent viscosity effect observed for the nanoparticle diffusion in polymer melts [36, 37]. Our results may be essential for developing suitable coarse-grain models to study biological systems and polymer nanocomposites filled with various types of carbon nanoparticles.

Dedication

We dedicate this paper to the memory of our teacher, Prof. Yu. Ya. Gotlib, from whom we have learned how the statistical physics methods can be applied to the intriguing challenges posed by polymer relaxation, and whose studies on polymer segmental mobility and heterogeneous dynamics always inspired us.

Acknowledgement

The authors thank Prof. E. A. Abad for his careful reading of the manuscript, as well as for very helpful comments and valuable suggestions. The simulations have been performed using the computational resources of the Institute of Macromolecular Compounds, Russian Academy of Sciences, Lomonosov-1 and Lomonosov-2 supercomputers at Moscow State University, and resources of the federal collective usage center "Complex for Simulation and Data Processing for Mega-science Facilities" at NRC "Kurchatov Institute" (http://ckp.nrcki.ru/).

References

1. Gotlib, Yu. Ya.; Darinskii, A. A.; Svetlov, Yu. E. Physical Kinetics of Macromolecules (Khimiya, Leningrad, 1986), in Russian.
2. Tsalikis, D. G.; Koukoulas, T.; Mavrantzas, V. G.; Pasquino, R.; Vlassopoulos, D.; Pyckhout-Hintzen, W.; Wischnewski, A.; Monkenbusch, M.; Richter D. Microscopic Structure, Conformation, and Dynamics of Ring and Linear Poly(ethylene oxide) Melts from Detailed Atomistic Molecular Dynamics Simulations: Dependence on Chain Length and Direct Comparison with Experimental Data. *Macromolecules* **2017**, V. 50, P. 2565–2584.
3. Stephanou, P. S.; Baig, C.; Mavrantzas, V. G. Projection of atomistic simulation data for the dynamics of entangled polymers onto the tube theory: calculation of the segment survival probability function and comparison with modern tube models. *Soft Matter* **2011**, V. 7, P. 380-395.
4. Solar, M.; Yelash, L.; Virnau, P.; Binder, K.; Paul, W. Polymer Dynamics in a Polymer-Solid Interphase: Molecular Dynamics Simulations of 1,4-Polybutadiene At a Graphite Surface. *Soft Materials* **2014, V.** 12, P. S80–S89.

5. Solar, M.; Mapesa, E. U.; Kremer, F.; Binder, K.; Paul, W. The dielectric α-relaxation in polymer films: A comparison between experiments and atomistic simulations. *Europhys. Lett.* 2013, V. 104, P. 66004.
6. Nazarychev, V.M.; Lyulin, A.V.; Larin, S.V.; Gofman, I.V.; Kenny, J.M.; Lyulin, S.V. Correlation between the High-Temperature Local Mobility of Heterocyclic Polyimides and Their Mechanical Properties. *Macromolecules* **2016**, 49, 6700-6710.
7. Falkovich, S.G.; Nazarychev, V.M.; Larin, S.V.; Kenny, J.M.; Lyulin, S.V. Mechanical Properties of a Polymer at the Interface Structurally Ordered by Graphene. *J. Phys. Chem. C.* **2016**, 120, 6771–6777.
8. Larin, S.V.; Glova, A.D.; Serebryakov, E.B.; Nazarychev, V.M.; Kenny, J.M.; Lyulin, S.V. Influence of the carbon nanotube surface modification on the microstructure of thermoplastic binders. *RSC Adv.* **2015**, 5, 51621-51630.
9. Lyulin, S.V.; Gurtovenko, A.A.; Larin, S.V.; Nazarychev, V.M.; Lyulin, A.V. Microsecond Atomic-Scale Molecular Dynamics Simulations of Polyimides. *Macromolecules* **2013**, 46, 6357–6363.
10. Glova, A. D.; Falkovich, S. G.; Dmitrienko, D. I.; Lyulin, A. V.; Larin, S. V.; Nazarychev, V. M.; Karttunen, M.; Lyulin, S. V. Scale-Dependent Miscibility of Polylactide and Polyhydroxybutyrate: Molecular Dynamics Simulations. *Macromolecules* **2018**, 51, P. 552–563.
11. Sharma, F. P.; Roy, S.; Karimi-Varzaneh, H. A. Validation of Force Fields of Rubber through Glass Transition Temperature Calculation by Microsecond Atomic-Scale Molecular Dynamics Simulation. *J. Phys. Chem. B* **2016**, 120, 1367–1379.
12. Forrey, C.; Saylor, D. M.; Silverstein, J. S.; Douglas, J. F.; Davis, E. M.; Elabd, Y. A. Prediction and validation of diffusion coefficients in a model drug delivery system using microsecond atomistic molecular dynamics simulation and vapour sorption analysis. *Soft Matter* **2014**, 10, 7480–7494.
13. Vogiatzis, G.G.; Theodorou, D.N. Multiscale Molecular Simulations of Polymer‐Matrix Nanocomposites or What Molecular Simulations Have Taught us About the Fascinating Nanoworld. *Arch. Computat. Methods Eng.* **2017**, P. 1–55, Springer Netherlands
14. Brini, E.; Algaer, E. A.; Ganguly, P.; Li, C.; Rodríguez-Ropero, F.; van der Vegt, N. F. A. Systematic coarse-graining methods for soft matter simulations – a review. *Soft Matter* **2013**, 9, 2108-2119.

15. Tripathy, M.; Deshpande, A. P.; Sunil Kumar, P. B. How Much Can We Coarse-Grain while Retaining the Chemical Specificity? A Study of Sulfonated Poly(ether ether ketone). *Macromolecular Theory and Simulations* **2016**, 25, 155–169.
16. Pandiyan, S.; Parandekar, P. V.; Prakash, O.; Tsotsis, T. K.; Basu, S. Systematic Coarse Graining of a High-Performance Polyimide. *Macromolecular Theory and Simulations* **2015**, 24, 513–520.
17. Salerno, K. M.; Agrawal, A.; Perahia, D.; Grest, G. S. Resolving Dynamic Properties of Polymers through Coarse-Grained Computational Studies. *Phys. Rev. Lett.* **2016,** 116, 058302.
18. Agrawal, V.; Holzworth, K.; Nantasetphong, W.; Amirkhizi, A. V.; Oswald, J.; Nemat-Nasser, S. Prediction of Viscoelastic Properties with Coarse-Grained Molecular Dynamics and Experimental Validation for a Benchmark Polyurea System. *Journal of Polymer Science, Part B: Polymer Physics* **2016**, 54, 797–810.
19. Karimi-Varzaneh, H. A.; van der Vegt, N. F. A.; Müller-Plathe, F.; Carbone, P. How Good Are Coarse-Grained Polymer Models? A Comparison for Atactic Polystyrene. *ChemPhysChem* **2012** ,13, 3428–3439.
20. Harmandaris, V. A.; Reith, D.; van der Vegt. N. F. A.; Kremer, K. Comparison Between Coarse-Graining Models for Polymer Systems: Two Mapping Schemes for Polystyrene. *Macromol. Chem. Phys.* **2007**, 208, 2109–2120.
21. Harmandaris, V. A.; Kremer, K. Predicting polymer dynamics at multiple length and time scales. *Soft Matter* **2009**, 5, 3920-3926.
22. Ohkuma, T.; Kremer, K. Comparison of two coarse-grained models of cis-polyisoprene with and without pressure correction. *Polymer* **2017**, 130, 88-101.
23. Root, S. E.; Savagatrup, S.; Pais, C. J.; Arya, G.; Lipomi, D. J. Predicting the Mechanical Properties of Organic Semiconductors Using Coarse-Grained Molecular Dynamics Simulations. *Macromolecules* **2016**, 49, 2886–2894.
24. Peters, B. L.; Salerno, K. M.; Agrawal, A.; Perahia, D.; Grest, G. S. Coarse-Grained Modeling of Polyethylene Melts: Effect on Dynamics. *J. Chem. Theory Comput.* **2017**, 13, 2890–2896.
25. D. Fritz; K. Koschke; V. A. Harmandaris; van der Vegt, N. F. A.; Kremer, K. Multiscale modeling of soft matter: scaling of dynamics. *Phys. Chem. Chem. Phys.* **2011**, 13, 10412–10420.

26. Lu, L.; Zheng, T.; Wu, Q.; Schneider, A. M.; Zhao, D.; Yu., L. Recent Advances in Bulk Heterojunction Polymer Solar Cells. *Chem. Rev.* **2015**, V. 115, P. 12666–12731.
27. Kausar, A. Progression from Polyimide to Polyimide Composite in Proton-Exchange Membrane Fuel Cell: A Review. *Polym. Plast. Technol. Eng.* **2017**, V. 56, P. 1375-1390.
28. Zheng, Z.; Li, F.; Liu, J.; Pastore, R.; Raos, G.; Wu, Y.; Zhang, L. Effects of chemically heterogeneous nanoparticles on polymer dynamics: insights from molecular dynamics simulations. *Soft Matter* **2018**, Advance Article.
29. Goswami, M.; Sumpter, B. G. Anomalous chain diffusion in polymer nanocomposites for varying polymer-filler interaction strengths. *Phys. Rev. E* **2010**, 81, P. 041801
30. Patti, A. Molecular Dynamics of Spherical Nanoparticles in Dense Polymer Melts. *J. Phys. Chem. B* **2014**, 118, P. 3731−3742.
31. Burgos-Mármol, J. J.; Álvarez-Machancoses, Ó.; Patti, A. Modeling the Effect of Polymer Chain Stiffness on the Behavior of Polymer Nanocomposites. *J. Phys. Chem. B* **2017**, 121, P. 6245–6256.
32. Smith, G. D.; Bedrov, D.; Li, L.; Byutner, O. A molecular dynamics simulation study of the viscoelastic properties of polymer nanocomposites. *J. Chem. Phys.* **2002**, 117, P. 9478-9489.
33. Hagita, K.; Morita, H.; Takano, H. Molecular dynamics simulation study of a fracture of filler-filled polymer nanocomposites. *Polymer* **2016**, 99, P. 368-375.
34. Shin, J.; Cherstvy, A. G.; Metzler, R. Self-subdiffusion in solutions of star-shaped crowders: nonmonotonic effects of inter-particle interactions. *New J. Phys.* **2015**, 17, 113028
35. Shin, J.; Cherstvy, A. G.; Metzler, R. Mixing and segregation of ring polymers: spatial
36. confinement and molecular crowding effects. *New J. Phys.* **2014**, V. 16, P. 053047.
37. Cai, L.-H.; Panyukov, S.; Rubinstein, M. Mobility of Nonsticky Nanoparticles in Polymer Liquids. *Macromolecules* **2011**, 44, 7853−7863.
38. Kalwarczyk, T.; Sozanski, K.; Ochab-Marcinek, A.; Szymanski, J.; Tabaka, M.; Hou, S.; Holyst, R. Motion of nanoprobes in complex liquids within the framework of the length-scale dependent viscosity model. *Adv. Colloid Interface Sci.* **2015**, 223, 55−63.
39. Volgin, I. V.; Larin, S.V.; Abad, E.; Lyulin, S. V. Molecular Dynamics Simulations of Fullerene Diffusion in Polymer Melts. *Macromolecules* **2017**, 50, 2207–2218.

40. Rühle, V.; Junghans, C.; Lukyanov, A.; Kremer, K.; Andrienko, D. Versatile Object-Oriented Toolkit for Coarse-Graining Applications. *J. Chem. Theory Comput.* **2009**, 5, 3211–3223.
41. http://manual.gromacs.org/documentation/5.1.1/manual-5.1.1.pdf
42. Xia, W.; Song, J.; N. K. Hansoge, ; R. Phelan Jr., F.; Keten, S.; Douglas, J. F. Energy Renormalization for Coarse-Graining the Dynamics of a Model Glass-Forming Liquid. *J. Phys. Chem. B* **2018**, V. 122, P. 2040–2045.
43. Xia, W.; Song, J.; Jeong, C.; Hsu, D. D.; R. Phelan Jr., F.; Douglas, J. F.; Keten, S. Energy-Renormalization for Achieving Temperature Transferable Coarse-Graining of Polymer Dynamics. *Macromolecules* **2017**, V. 50, P. 8787–8796.
44. Li, Z.; Lee, H. S.; Darve, E.; Karniadakis, G. E. Computing the non-Markovian coarse-grained interactions derived from the Mori–Zwanzig formalism in molecular systems: Application to polymer melts. *Journal of Chemical Physics* **2017**, V. 146, P. 014104.